DOCUMENT

Deliverable Number	**D4.1**	Due Date	31/01/2015
Issued by WP/Task	**WP4/T4.1**	Actual Date	06/02/2015
Dissemination Level	**PUBLIC**	Pages	36
		Appendices	none

PROJECT

Grant Agreement No.	606645
Acronym	RPB HealTec
Title	ROAD PAVEMENTS & BRIDGE DECK HEALTH MONITORING / EARLY WARNING USING ADVANCED INSPECTION TECHNOLOGIES
Call	**FP7-SME-2013**
Funding Scheme	BSG-SME

Deliverable D4.1

ACU procedures – guidelines and essential parameters for ACU (modelling)

AUTHORS

	CITY	P. LIATSIS, A.UUS, P.SHAW
	NARDONI	G. NARDONI

APPROVAL

Workpackage Leader	NARDONI	G. NARDONI
Technical Coordinator	CERTH	S. MOUSTAKIDIS
Project Coordinator	CITY	P. LIATSIS

AUTHORIZATION

Project Officer	REA	K. AMOLOCHITIS

CONSORTIUM

	Beneficiary name	Country
1	City University London (CITY)	UK
2	I&T Nardoni Institute S.R.L. (NARDONI)	Italy
3	MET GEOENVIRONMENTAL (METGEO)	UK
4	Global Digital Technologies (GDT)	Greece
5	IRIS Thermovision (IRIS)	Netherlands
6	Autostrada del Brennero SpA Brennerautobahn AG (BRENNERO)	Italy
7	Vrancea County Council (CJ VRANCEA)	Romania
8	CENTER FOR RESEARCH & TECHNOLOGY HELLAS (CERTH)	Greece
9	Center for Research Technology & Innovation (CETRI)	Cyprus

REVISION HISTORY

VER.	DATE	PAGES	NOTES	AUTHORS (partners)
01	10/11/2014	All	First draft (structure)	P. Liatsis (CITY), P. Shaw (CITY), A. Uus (CITY)
02	20/11/2014	All	Input from the experts	G. Nardoni (NARDONI), S. Moustakidis (CERTH)
03	15/12/2014	All	Specification of the FE model and preliminary results	P. Shaw (CITY), A. Uus (CITY)
04	17/01/2015	All	FE simulation results for the parametric study	P. Shaw (CITY), A. Uus (CITY)
05	25/01/2015	All	Corrections, introduction and summary sections	P. Liatsis, P. Shaw (CITY), A. Uus (CITY)
06	02/01/2015	All	Additional FE simulations and corresponding analysis	P. Shaw (CITY), G. Nardoni (NARDONI), A. Uus (CITY)
07	05/01/2015	All	Final draft with input from Coordinator	P. Liatsis (CITY)
Final	06/01/2015	All	Approved	P. Liatsis (CITY)

EXECUTIVE SUMMARY

The overall objective of WP4 is to develop an advanced ACU system that can detect defects such as subsurface delaminations with sufficient accuracy and at high acquisition rates, more specifically:

1. To develop an appropriate ACU system;
2. To determine the essential procedure parameters;
3. To develop the sensors and integrated sensor system capable of delivering reliable information by addressing the deterioration of the signal through the air.

As part of task T4.1 "Investigation of essential ACU parameters", the purpose of D4.1 is to investigate the possible impact on air coupled ultrasonic wave transmission in the context of the geometrical configuration of the transducers, transducer operating frequency and voltage, near field position, delamination location and material characteristics. To achieve this, FE models were created in order to specify the optimal values and limits of the system parameters in terms of detection of subsurface delaminations and sensitivity to surface defects. The results of this study will be further analysed and validated during the laboratory tests of the ACU equipment.

TABLE OF CONTENTS

ABBREVIATIONS

AASHTO	American Association of State Highway and Transportation Officials
ACU	Air-Coupled Ultrasound
ADC	Analogue to Digital Convertor
CCU	Central Control Unit
COST	European Cooperation in Science and Technology
DOT	Department of Transportation
EUs	End Users
GMPC	Gas Matrix Piezoelectric Composites
GPR	Ground Penetrating Radar
GPS	Global Positioning System
GUI	Graphical User Interface
FEM	Finite Element Modelling
HMA	Hot Mix Asphalt
IRT	Infrared Thermography
LWB	Lamb Wave Beam
NCU	Non-Contact Ultrasound
NDT	Non-Destructive Testing
QC/QA	Quality Control and Acceptance
REA	Research Executive Agency
SHRP	Strategic Highway Research Program
SNR	Signal to Noise Ratio
WP	Work Package

1 INTRODUCTION

In Europe, dry- , water- , and oil- coupled ultrasound are standard test methods for structural concrete inspection for detection of internal defects and delaminations, changes in material properties, estimation of strength and uniformity, etc. A number of research works describe the use of ultrasonic techniques for HMA QC/QA. The recently emerged air-coupled ultrasound (also known as non-contact ultrasound / NCU) NDT technology is not limited by contact coupling (the main limitation of classical US), with modern systems capable of producing relatively high resolution results. The fact that ACU does not require the initial preparation of the surface also significantly simplifies the inspection procedure and eliminates possible operator errors. Lack of spatial restrictions allows inspection of large areas, flexible orientation of transducers, and high inspection speed. In this context, the application of ACU in pavement and bridges inspection can prove to be potentially efficient, as it can be performed over kilometres of road surfaces with relative ease.

The main constraint for the application of ACU is low SNR as only a small portion of the ultrasonic signals is transmitted through the inspected material due to the high impedance mismatch between air and solids. However, new materials used in ACU transducers, dedicated equipment, and advanced signal processing have recently proven to be efficient enough to inspect structural concrete and asphalt samples with penetration depths of 20 cm or higher [1,19,7,20]. As the technology is relatively new, the state of the art in ACU inspection of concrete and HMA is limited, with the US Transportation Research Board reporting ACU as a promising method in highway inspection [21].

In his PhD thesis, Gräfe [1] demonstrated that pitch-catch ACU inspection in the 100 kHz frequency range has high potential as a NDT method for inspection of large concrete structures. Figure 1.1 illustrates single-side 85 kHz ACU inspection of a 20 cm thick concrete sample with a side-drilled hole and the measured C-scan [1].

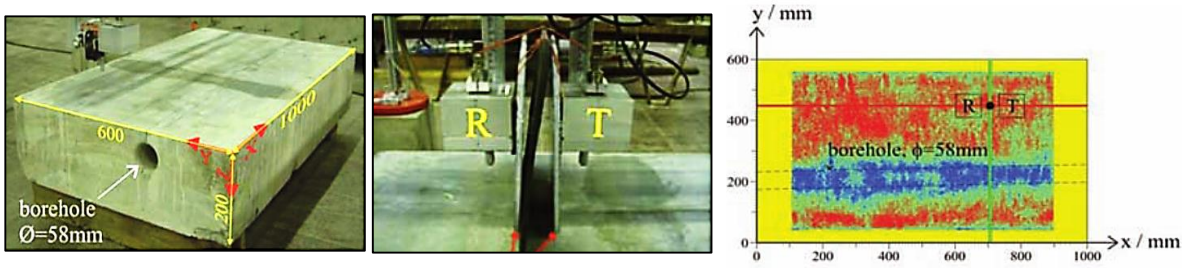

a. 20 cm thick concrete sample with a borehole *b. single-side ACU transducer configuration* *c. C-scan at z = 200 mm (backwall)*

Figure 1.1 ACU inspection of 20 cm thick concrete sample [1]

The following two commercially available ACU systems have been reported to be used for concrete and HMA inspection: ULTRAN SecondWave™ M510x NCU system [6] and USPC 4000 AirTech DR.HILLGER [7]. For instance, Figures 2.2.b-c show the B-scan of a 76 mm thick HMA sample with uneven mix and the B-scan of a 200 mm thick concrete with variations in texture [20].

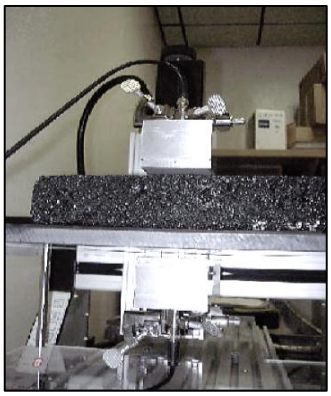

a. ACU inspection of 70 mm HMA sample [23]

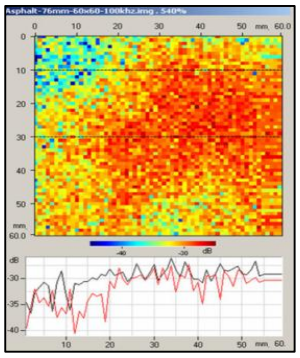

b. B-scan: 76 mm HMA with uneven mix / 100 kHz [20]

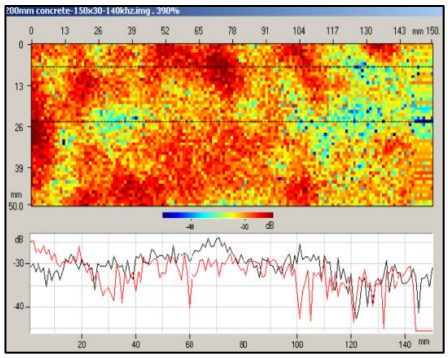

c. B-scan: 200 mm thick concrete with variations in texture / 140 kHz [20]

Figure 1.2 Inspection of concrete and HMA samples with NCU ULTRAN transducers [20]

The two sided ACU inspection of a 20x20x50 cm concrete sample with gravel nest using the USPC AirTech 4000 DR.HILLGER system [7] is presented in Figure 1.3 and the associated C-scan clearly shows that the signal amplitude decreases more than 18 dB at the gravel region.

a. concrete sample with 10cm gravel nest and the USPC 4000 AirTech system

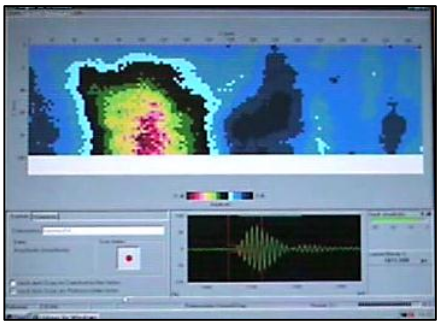

b. C-scan of the concrete sample (Hillgus software)

Figure 1.3 Inspection of concrete sample (20x20x50 cm) with the USPC 4000 AirTech DR.HILLGER system [7]

Purnell et al. [18,22] demonstrated the feasibility of ACU as a method for inspection of concrete material properties (humidity and aggregate content) on a 7.5 cm thick concrete plate. Kee and Zhu [23] successfully demonstrated the application of ACU in the measurement of surface cracks depth in concrete structures (based on surface waves' analysis). In his PhD thesis, Dunning [17,19] showed the feasibility of low frequency ACU as applied to HMA mix design quality control and detection of density changes.

It is rather difficult to predict the spatial resolution of ACU inspection as it is directly determined by the material properties, size of the inspected object, frequency, acquisition mode, sampling rate, and the transducer geometry. Frequencies used for concrete inspection generally vary in the 50 – 150 kHz range. It was reported that 1 m is the achievable penetration depth for ACU through-transmission inspection of concrete structures [6,7], while the effective resolution of ACU images highly depends on the problem domain and in general ranges from 1 to 30 mm [13-14]. However, these figures might differ for single-side pavement inspection as concrete and HMA are considered as “difficult” for ACU

inspection being made of highly attenuating and scattering material [15] and because of the initially unknown structure thickness.

1.1 ACU system components

The main techniques used to improve the system performance with respect to low SNR include the use of advanced transducers with matching impedance layers, high voltage pulses for transducer excitation, low-noise preamplifier and band pass filters in the receiving transducer, choice of optimal frequency and the geometrical configuration of the transducers (angle, separation distances), as well as advanced signal processing techniques.

Figure 1.4 shows a typical ACU system consisting of (i) high power function generator (pulser), (ii-iii) transmitting and receiving ACU transducers /or transducer arrays, (iv) preamplifier, (v-vi) analogue and digital signal processing equipment (ADC and filters), and (vii) CPU for control, data recording, image processing, storage and analysis.

The CPU is used for setting and tuning all acquisition parameters, control of time and motion synchronized acquisition, storage, signal processing, analysis and display of the results. It transfers the acquisition settings, such as frequency, pulse type and width, and the pulser driving voltage, to the function generator. The function generator transmits electrical pulses to the transducer, which are transformed to focused ultrasound signals.

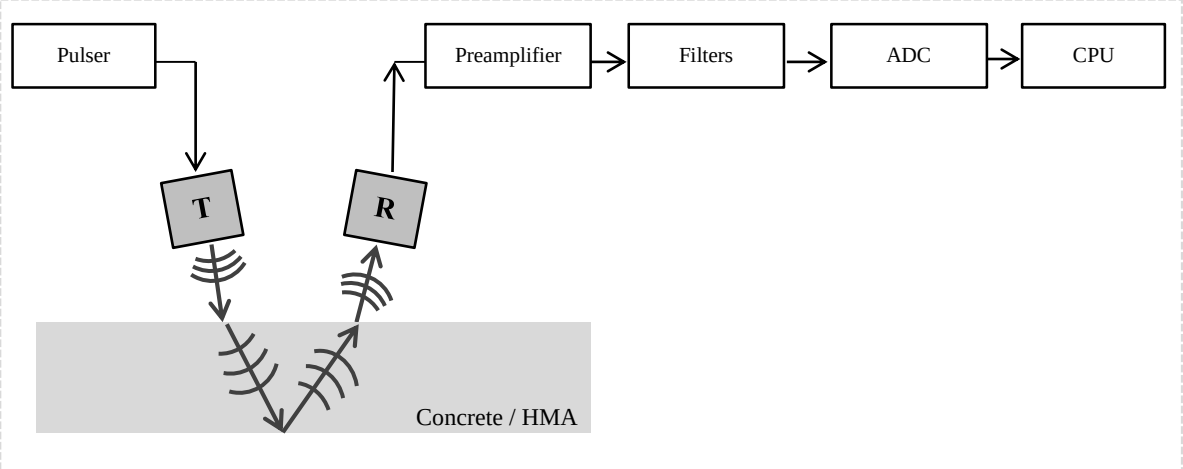

Figure 2.1 ACU system components

At the receiving side, the signal detected at the transducer is passed to the low-noise amplifier and band pass analogue filters. ADC converts the analogue signal to digital form with a specified sampling rate. System components are connected through high-speed interfaces. At the same time, besides the equipment quality, the system performance and detection of defects directly depends on the system settings, i.e., choice of optimal frequency, position and angle of transducers, and signal excitation mode and power, all of which in its turn depend on the material properties and structure thickness. In other words, systematic tuning of the system parameters for the specific application has to be conducted through a series of experiments. Though the system will be operating at relatively low frequencies, in order to overcome the low SNR it is preferable to have as high a bit depth as possible.

It is also preferable for the ADC to have a high sampling rate as so that oversampling can be implemented to increase the SNR.

1.2 System limitations and requirements

A number of factors that can impede implementation of the proposed ACU system for pavement inspection as well as decrease the accuracy of defect detection: (i) high air/HMA impedance mismatch, (ii) high inspection speed, (iii) vehicle dynamics, (iv) weather conditions (high temperatures, humidity and turbulence), (v) road surface irregularities, (vi) external noise sources (e.g., traffic), etc.

The main risk is related to the high impedance mismatch between air and road surface materials (HMA and concrete) as well as the signal at the transducer-air interfaces (however, use of modern transducers significantly lowers the signal loss). In any case, the detected waves will have a low SNR, but optimal system settings, transducer geometry, signal processing, and filtering can be used to improve the quality of the results.

Kichou et al. [15] showed that ACU transducers are highly sensitive to the angular orientation of the surface structure in terms of the LWB deviation and amplitude losses. Irregular/damaged pavement surfaces might lead to decreased signal amplitude and erroneous results, as the received signals will mask the signals from the subsurface defects. Therefore, it is important to take into account this problem when inspecting large structures. In addition, the incidence angle directly affects the signal propagation and has to be carefully adjusted [16].

Another possible risk is related to the difficulty in distinguishing between various defect types. The presence of defects in the inspected material causes diffraction of the ultrasound signal around the defect, which is detected as a reduction of the signal amplitude, change of the signal time of flight, or discontinuity. However, defects such as voids and buried objects can produce similar changes in the signal.

Considering the required depth of penetration for surface pavement layers (10-16 cm for highways, and 11–20 cm for bridges) and the highly inhomogeneous and granular nature of HMA and concrete [16], the optimal inspection frequency should not exceed the 75 – 150 kHz range, which results to lower resolution and potentially lower detection accuracy.

The majority of ACU transducers are sensitive to water due to the materials used as matching layers. For example, in the case of the standard ULTRAN transducers, humidity greater than 90% is not recommended, however specialist “environment-proof” versions are less sensitive [6]. In addition, the acoustic impedance of humid air under high temperatures is approximately 5% lower. The “ideal” conditions for ACU inspection are in dry cold air. In relation to the “wet” road surface conditions however, Berriman et al. investigated the effect of humidity on ACU inspection of concrete and the results showed that the speed of sound is higher in concrete samples with high water content [18].

2 THEORETICAL MODEL

As a part of Task 4.1 "Investigation of essential ACU parameters", various system configuration parameters require preliminary investigation with respect to the specifics of the application of ACU in single-side HMA inspection.

FEM analysis has been extensively used for numerical simulation of ultrasound propagation in various materials and also in ACU system design. For instance, the CIVA NDT engineering software [24] provides instruments for professional design of ultrasound transducers (and phased arrays) and corresponding FEM ultrasound simulation for optimisation of the transducer configuration and prediction of interaction of ultrasound with various materials and flaws. A number of research groups performed FEM studies of ultrasound propagation in air-solid interfaces. Ke et al. [25] developed a 3D FEM model of an ACU NDT system that showed good agreement between numerical predictions and experimental measurements for ACU inspection of aluminium and glass–polyester composite plates with internal defects. Dobie et al. [26] and Delrue et al. [27] proposed the use of 2D and 3D FEM simulations of Lamb wave propagation for optimisation of the design of the ACU pitch-catch scanner.

Based on the specifications and limits for the parameter values obtained from the ACU equipment specifications [1, 6, 7, 12, 19], a 3D FEM model of the proposed system was developed in order to investigate the system's feasibility to detect subsurface defects and the optimal system configuration. This discretised model is defined over pressure acoustics (frequency domain), solid mechanics domains along with the coupling at solid and air interface boundaries and piezoelectic effects. The desciption of the governing equations and the FEA solver specific discretisation methods can be found in [2].

$$\nabla \cdot \left(-\frac{1}{\rho}(\nabla p) \right) - \frac{\omega^2 p}{\rho c^2} = 0 \qquad (2.1)$$

where ρ is the density of the medium, ω is the angular frequency, and c is the speed of sound.

The following parameters of the ACU system were investigated with respect to the detection of delaminations: (i) nearfield positions, (ii) angle of incidence, (iii) operating frequency, (iv) excitation voltage and, (v) shield-surface distance.

Being highly interrelated the values of these parameters were preliminary estimated based on the calculation of the near field and critical angles, while their optimal values were derived by analysis of their impact on the system's efficiency in the detection of delaminations. Additional requirements for the ACU system geometry are the safety of the equipment (the transducers cannot be too close to the surface), and availability of the transducers of specified diameter/frequency on the market.

2.1 Case study – test slab geometry

The test pavement model used in the experiments is 0.100 × 0.100 m in size with varying length depending on the geometry setup to reduce the computational costs. The in-depth HMA layer structure is based on the BRENNERO pavement design [12] (40-mm surface, waterproof bituminous membrane, and 60-mm binder layers), shown in Figure 2.1. The locations of the modelled subsurface delaminations, surface opening cracks, and potholes are depicted by red lines (these were chosen in accordance with the most frequently reported locations). The characteristics of utilised HMA, concrete, and bitumen materials are based on the standard data from the FEM solver [2].

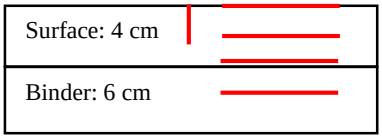

Figure 2.1 Test slab model layout (surface layer of the BRENNERO pavement design) with delamination locations

2.2 FE model description

Modelling of the ACU single-side inspection of this test slab implies development of the corresponding, real-size 3D FE model for the solution of the ultrasound propagation through the specified geometries. In summary, this model is based on the physics defining the acoustics and piezoelectric effects over the discretised 3D models of the test slab, air blocks and a pair of transmitting and receiving ACU transducers.

The simulations were conducted using the commercially available COMSOL Multiphysics FEA Software package. The general characteristics of the developed ACU FE model are as follows:

- The geometry of the 3D model, as depicted in Figure 2.2, includes the following components: air, concrete/HMA slabs, transducers, and shield.
- Subsurface delaminations and surface opening cracks were geometrically modelled as a thin layer with low modulus HMA, or as air- and water-filled voids (splits) with varying depth.
- Spatial discretisation of the model domains was performed in accordance with the wavelength requirement to the maximum mesh element size [2].
- The idealised ultrasound transducers of the specified diameters (30 and 50 mm) were modelled as PZT-H5 piezoelectric components with a low impedance λ/4 thickness matching layer.
- The value of the baseline pulse signal frequency was chosen at 75kHz based on the results of Gräfe [1] and Dunning [19] and limits provided by the ACU vendors [6-11].
- A sound absorbing boundary was used for the shield between the transducers to eliminate the effects of signal reflections.
- The preliminary geometrical configuration of the transducers (angle and separation distances) is based on the values specified for the ACU system for single-sided inspection of concrete by Gräfe [1].
- The simulations were performed in the frequency domain to reduce computational costs.
- Far field calculation boundaries were used along the top, bottom, and side edges of the model domain to eliminate the reflecting waves.

– The results of the parametric study are quantitatively and qualitatively represented as cross sections of the ultrasound propagation (acoustic pressure levels) through the test slabs and impulse response (Vpp) on the receiving transducer.

Figure 2.2 presents an example of geometry setup and results of the computed acoustic pressure levels distribution.

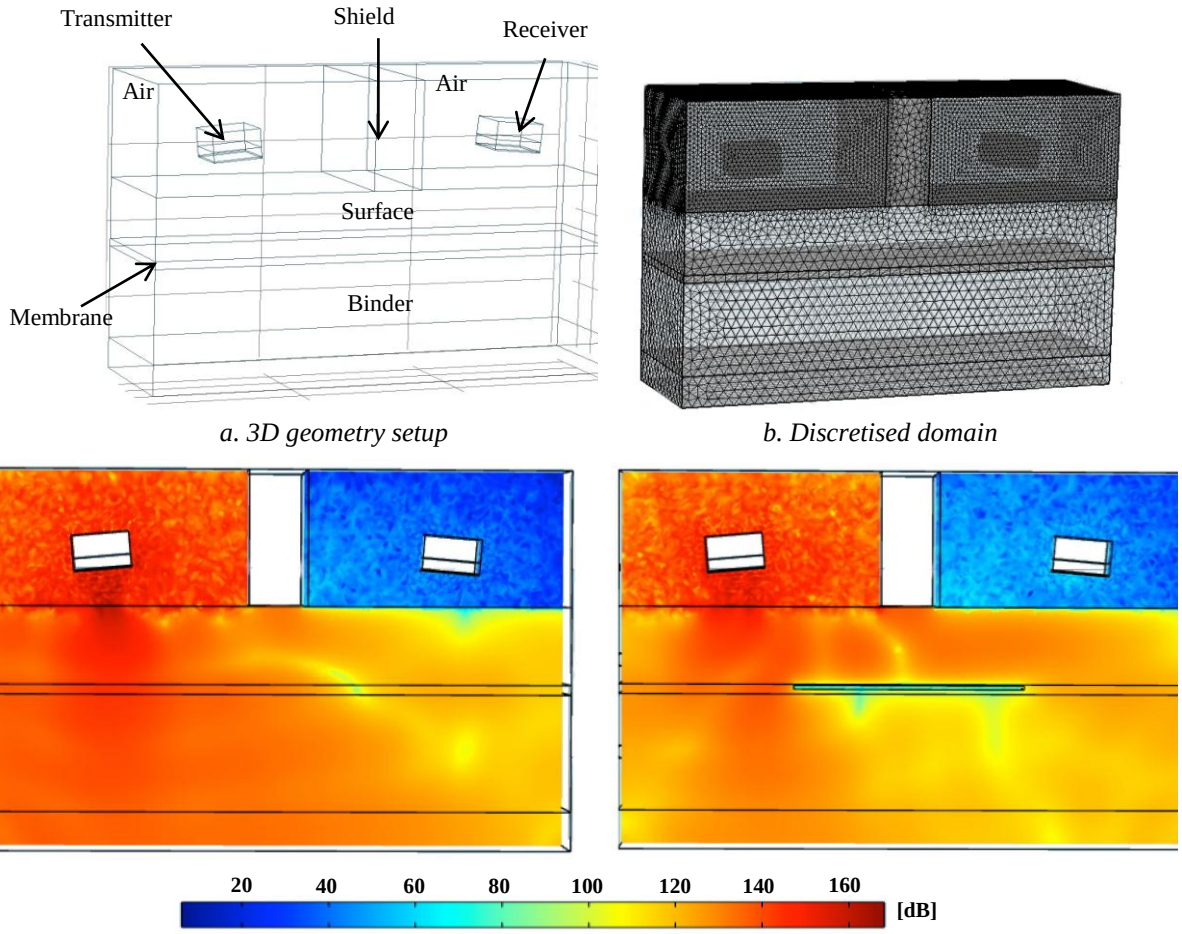

a. 3D geometry setup

b. Discretised domain

c. Cross sections of the computed acoustic pressure levels [dB] for two cases (75kHz): baseline HMA surface layers with and without subsurface delamination

Figure 2.2 An example of 3D FE model setup and the computed ACU propagation through the HMA test slab

As mentioned above, the goal of this case study is the assessment of the impact of the essential ACU system parameters on detection of subsurface pavement defects. Table 2.1 summarises the system parameters investigated during the FE simulations for the specified case study. The limits for the values are based on the preliminary evaluation of the system parameters and information from the vendors [6-11].

Table 2.1. ACU system parameters

	Parameters	**Values**
Transducers	active area shape	round
	diameter	30
Geometrical configuration	transducer-surface distance	30 - 70 mm
	transducer angle	$3 – 9^0$
	transducer-transducer distance	90 - 95 mm
	shield –surface distance	0 - 5 mm
Pulser	frequency	50 - 100 kHz
	voltage	200 – 500 V
Delamination	depth	20/30/40/60/80 mm
	filling	air / water / low density HMA(stripped)
	severity of debonding (height)	2 – 5 mm
Surface defects	surface opening crack/pothole	2x7 , 7x10, 30x10 mm width/depth

2.3 Geometrical configuration

The geometrical configuration parameters for each of the cases considered were based on the calculation of the near field with respect to the required transducer operating parameters, focus point, and inspection depth.

Focal length/Near field: Near field is defined as the distance at which the pressure waves combine to form a roughly uniform wave front. It is after this point that the signal is considered to be well behaved and at its maximum strength. The near field (N) is dependent on the diameter of the active area (D), the frequency of the signal (F) and the wave velocity in the medium (V). The near field imposes constraints on the distance between the surface of the material to be inspected and the transducers.

$$N = \frac{D^2 F}{4V} \tag{2.2}$$

Transducer/Receiver Geometry: Snell's law was used to determine the positioning of the transducer and receiver relative to each other. To do this, the propagation of both longitudinal and transverse waves, and associated critical angles were determined. The first critical angle determines the point at which there is total reflection of the longitudinal wave. The second critical angle determines the point at which there is total reflection of the transverse wave.

Refraction (Snell's Law):

$$\frac{Sin\,\theta_1}{V_{L_1}} = \frac{Sin\,\theta_2}{V_{L_1}} \tag{2.3}$$

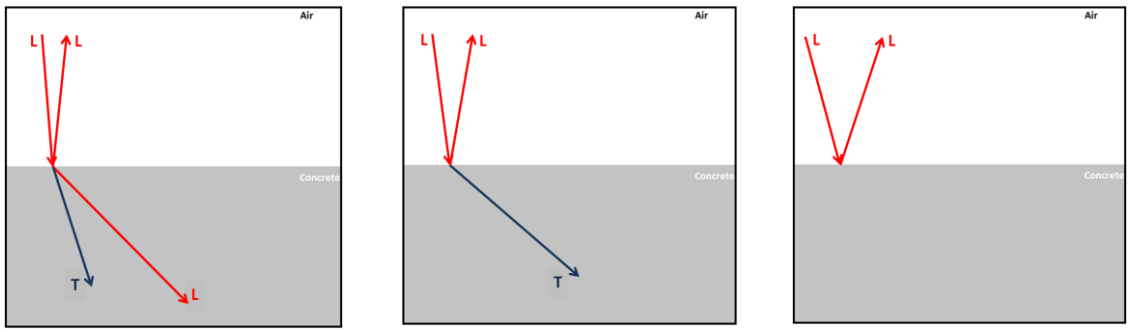

a. Perpendicular < Θ < First Critical Angle *b. First Critical Angle < Θ < Second Critical Angle* *c. Θ > Second Critical Angle*

Figure 2.3 Requirements for the angle of incidence

2.4 Simulation results

The following subsections present the simulation results for the specified cases.

2.4.1 CASE I: Baseline study

The base line for this study was created as a point of reference to investigate the effects of parameter changes to the ACU system performance.

From the list of suppliers the "AirTech 75" [7] transducers were identified as being optimised about the centre of the estimated ACU system parameters listed in Table 2.1. Based on the material characteristics the first and second critical angles were then calculated with respect to the propagation between the air and the asphalt concrete sample. It was decided that the transducer geometry for this case would be optimised for the propagation of transverse waves, as indicated by Gräfe's results in ACU concrete inspection [1]. So as to minimise the transducer distance, the angle was set just above the first critical angle. From the transducer specifications, the near field was calculated and the height from surface was set so that the wave would reach the surface at the near field distance along the wave vector [5]. The delamination was modelled at the interface within the bituminous membrane, which separates the surface and the binder within the HMA media. From these parameters, it was then possible to calculate the wave propagation by Snell's Law and set the transducer separation distance.

Baseline case	
Active Area Diameter (mm)	30
Frequency (kHz)	75
Angle (Degrees)	5
Near Field (mm)	49.17
Near Field Depth from Surface (mm)	0
First Critical Angle (Degrees)	4.93
Second Critical Angle (Degrees)	6.93
Delamination Depth (mm)	-40
Inspection depth (mm)	-40
Transducer Separation (mm)	92.35
Height from surface (mm)	48.98
Excitation voltage (V)	300

a. Case setup

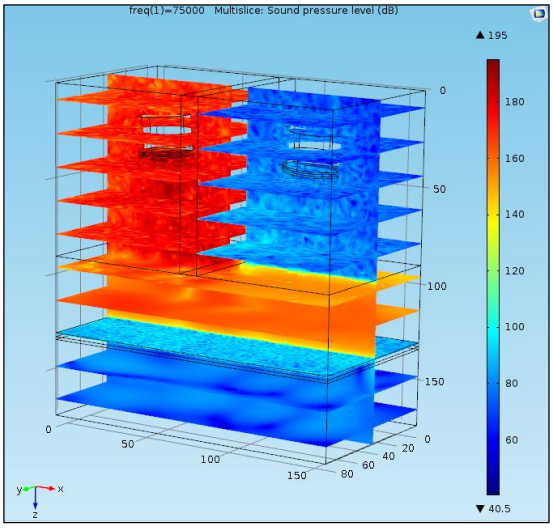

b. Computed acoustic pressure levels

Figure 2.4 Baseline study

2.4.2 CASE II: Near Field Study

The near field study investigates the effect of the near field parameter on the received signal (Vpp) with respect to its distance from the inspection surface. As the speed of sound in the material for inspection is significantly higher than in air, the near field moves below the surface and the wave focuses faster. This means that as the near field moves into the media for inspection the distance at which the wave becomes well behaved and at its peak intensity decreases. Figures 2.5-6 show the impact of the near field position variations (i.e., transducer-surface distance) on the impulse response for the cases with and without subsurface delamination. An air-filled 2mm height delamination is located 40 mm below the surface within the bituminous membrane, which is one of the most prominent delamination locations due to debonding. As the near field tends towards below the surface, the impulse response increases. However, safety requirements limit the transducer height from the surface and from these results it was decided that 39 mm will be the optimal distance for the present transducer configuration (Figure 2.6.g-h).

Near Field Study	
Active Area Diameter (mm)	30
Frequency (Hz)	75000
Angle (Degrees)	5
Near Field (mm)	49.17
Near Field Depth from Surface (mm)	+20 to -2.1
First Critical Angle (Degrees)	4.93
Second Critical Angle (degrees)	6.93
Delamination Depth (mm)	-40
Inspection depth (mm)	-40
Transducer Separation (mm)	95.8 to 89.0
Height from surface (mm)	68.9 to 29.9
Excitation voltage (V)	300

a. Case setup

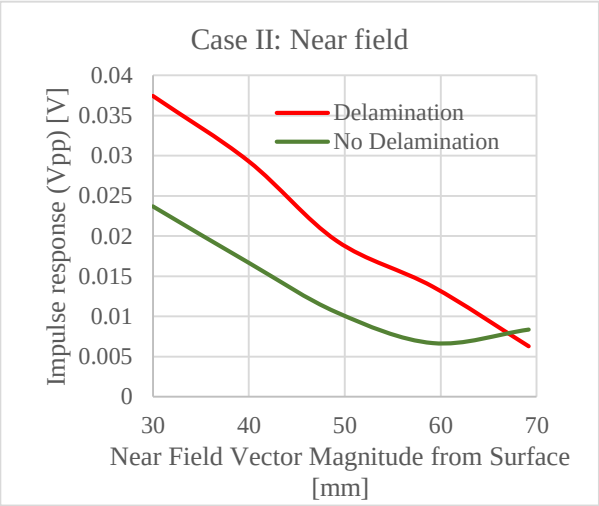

b. Excitation voltage vs. Impulse response at the receiver (Vpp)

Figure 2.5 Investigation of the impact of the excitation voltage

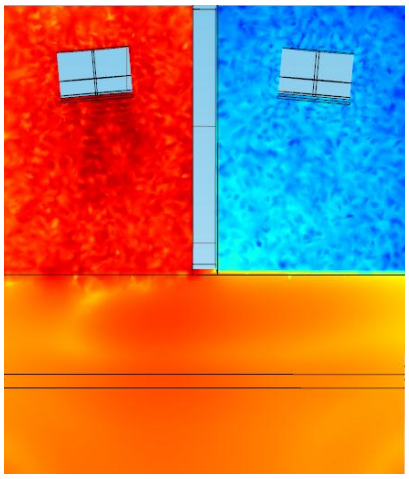

a. Near field 20mm from surface/ no delamination [dB]

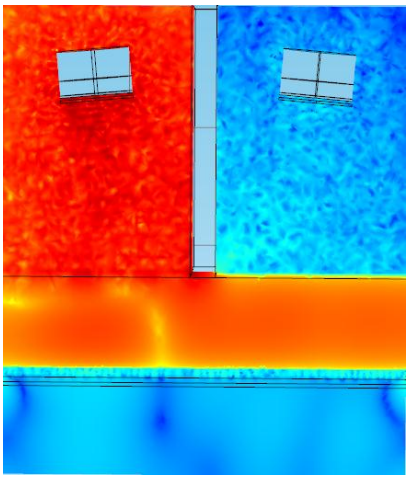

b. Near field 20mm from surface / 40 mm delamination [dB]

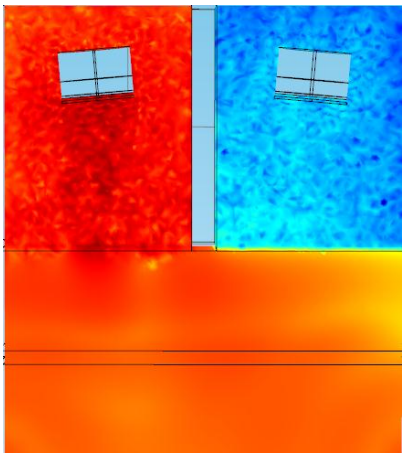

c. Near field 10mm from surface / no delamination [dB]

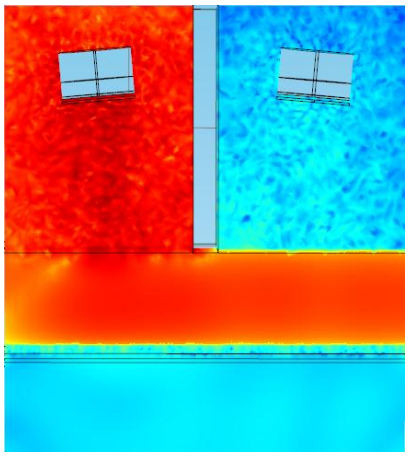

d. Near field 10mm from surface / 40 mm delamination [dB]

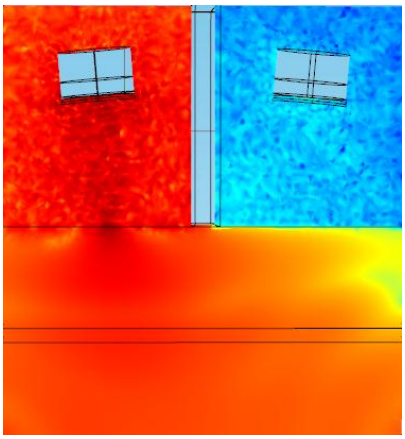

e. Near field 0mm from surface / no delamination [dB]

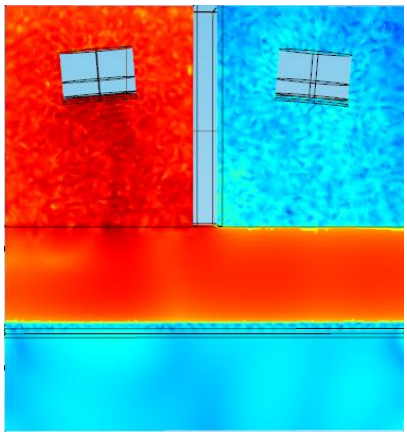

f. Near field 0mm from surface / 40 mm delamination [dB]

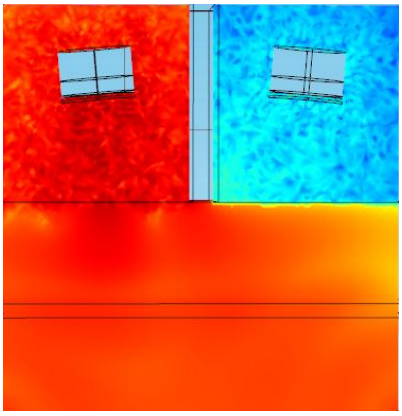

g. Near field -1.1mm from surface / no delamination [dB]

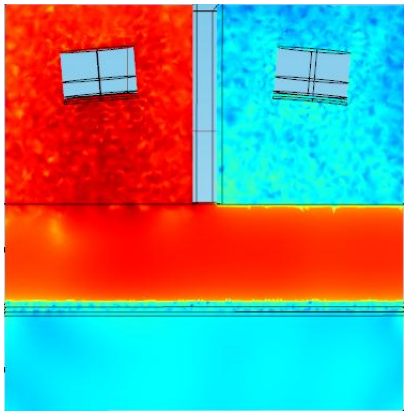

h. Near field -1.1mm from surface / 40 mm delamination [dB]

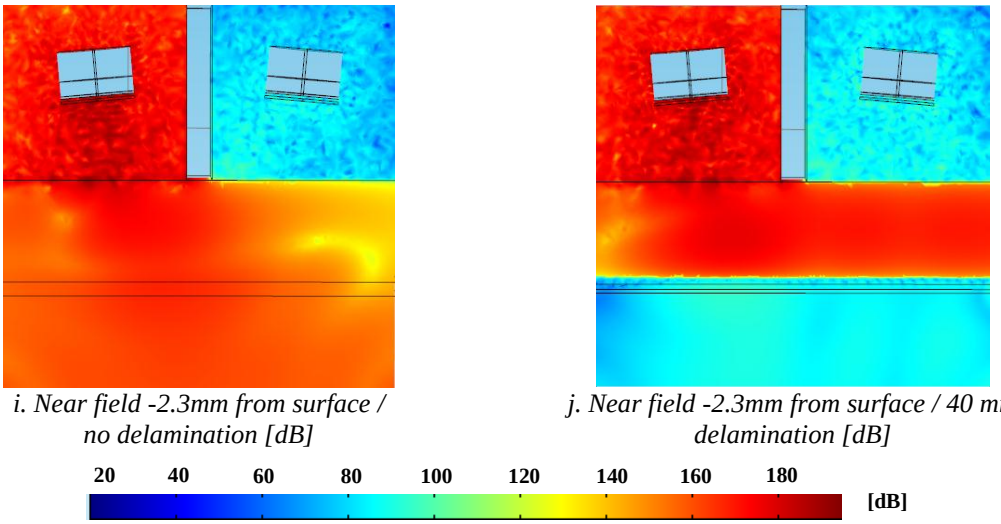

i. Near field -2.3mm from surface / no delamination [dB]

j. Near field -2.3mm from surface / 40 mm delamination [dB]

Figure 2.6 Investigation of the impact of the transducer-surface (TS) distance

2.4.3 CASE III: Operating frequency study

The operating frequency affects both the transmission magnitude and the near field parameter. Modern ACU transducers have a matching layer which is optimised for wave transmission at a specific operating frequency. As the operating frequency deviates away from the optimised frequency value, transmission decreases significantly. For each of these tests, the transducer matching layer was remodelled for optimal transmission at ~¼ λ. As the frequency increases, the near field distance increases. For comparison purposes, the geometrical configuration was adjusted for each of the test cases so that the wave would reach the surface at the near field distance.

Figures 2.7-8 show the computed acoustic pressure levels for three inspection frequencies, i.e., 50, 75, and 100 kHz. An inspection frequency of 75 kHz was chosen as the baseline following the results of Grafe [1] and Dunning [19] for inspection of concrete and HMA as well as the commercial availability of ACU transducers [6,7]. Although providing higher resolution, due to high absorption and scattering (which are even higher for porous sound-absorbing HMA), frequencies higher than 100 kHz were not considered. As can be observed in Figure 2.7.b, the highest difference in the impulse response between the cases with and without delamination is at 75 kHz. However, due to the idealised nature of the FE model of the transducers, this choice will be verified during the laboratory tests with various transducers.

Operating frequency study	
Active Area Diameter (mm)	30
Frequency (kHz)	50 - 100
Angle (Degrees)	5
Near Field (mm)	32.65 - 65.56
Near Field Depth from Surface (mm)	0
First Critical Angle (Degrees)	4.93
Second Critical Angle (Degrees)	6.93
Delamination Depth (mm)	-40
Inspection depth (mm)	-40
Transducer Separation (mm)	89.49 - 95.21
Height from surface (mm)	32.65 - 63.10
Excitation voltage (V)	300

a. Case setup

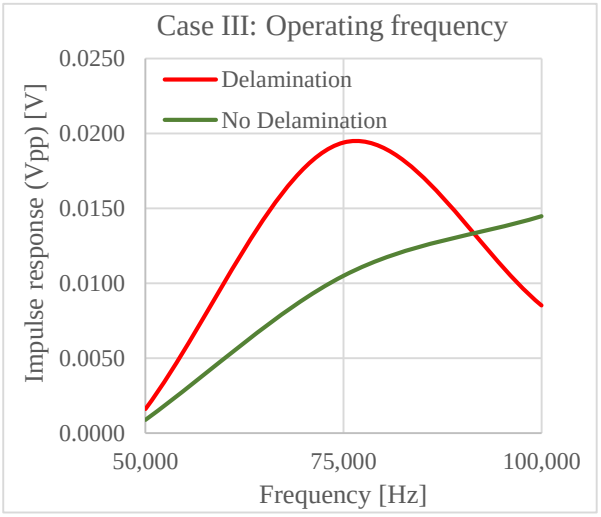

b. Inspection frequency vs. Impulse response at the receiver (Vpp)

Figure 2.7 Investigation of the impact of the inspection frequency

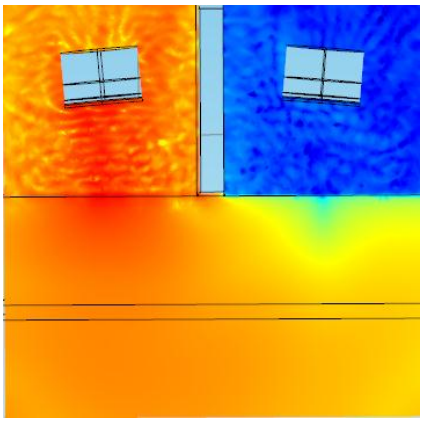

a. 50 kHz frequency / no delamination [dB]

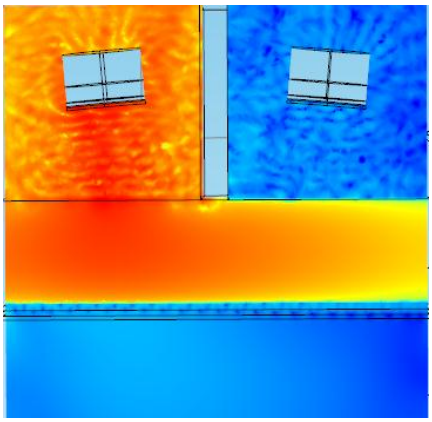

b. 50 kHz frequency / 40 mm delamination [dB]

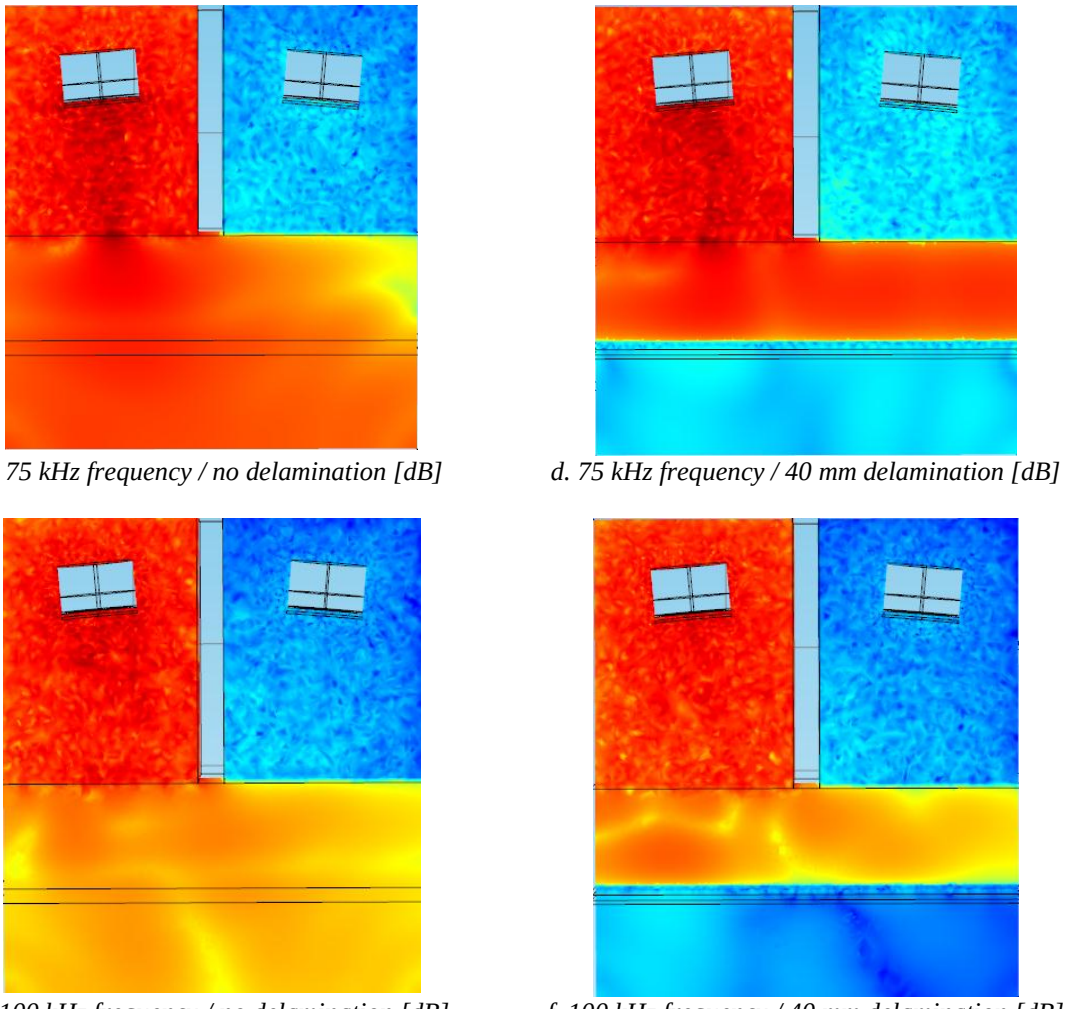

c. 75 kHz frequency / no delamination [dB]

d. 75 kHz frequency / 40 mm delamination [dB]

e. 100 kHz frequency / no delamination [dB]

f. 100 kHz frequency / 40 mm delamination [dB]

Figure 2.8 Investigation of the impact of the inspection frequency

2.4.4 CASE IV: Operating voltage study

The operating voltage study investigates the effect on the received signal as the transmitter voltage parameter is increased. The computed acoustic pressure levels in Figure 2.10 and the impulse response in Figure 2.9 demonstrate the impact of increasing the excitation voltage. While this increases the signal amplitude, the relative difference between the cases with and without delamination remains approximately the same. All other parameters for this study are based on the near field test case “g” (Figure 2.6.g).

Baseline case	
Active Area Diameter (mm)	30
Frequency (Hz)	75000
Angle (Degrees)	5
Near Field (mm)	41.1
Near Field Depth from Surface (mm)	0
First Critical Angle (Degrees)	4.93
Second Critical Angle (Degrees)	6.93
Delamination Depth (mm)	-40
Inspection depth (mm)	-40
Transducer Separation (mm)	90.76
Height from surface (mm)	39.85
Excitation voltage (V)	200-500

a. Case setup

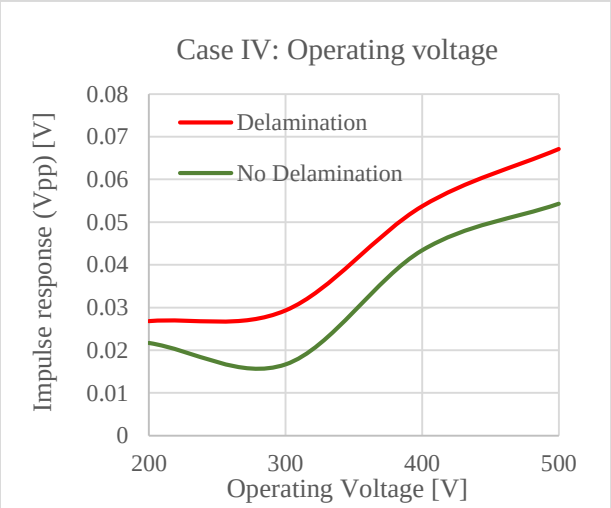

b. Excitation voltage vs. Impulse response at the receiver (Vpp)

Figure 2.9 Investigation of the impact of the excitation voltage

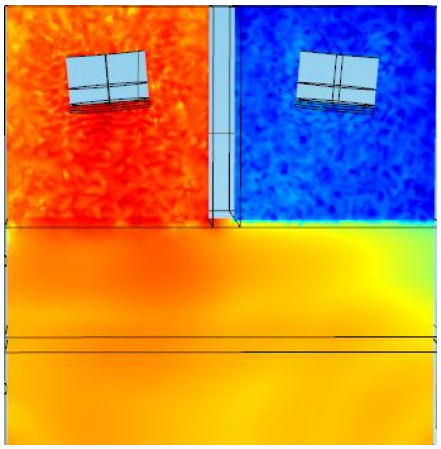

a. 200 V / no delamination [dB]

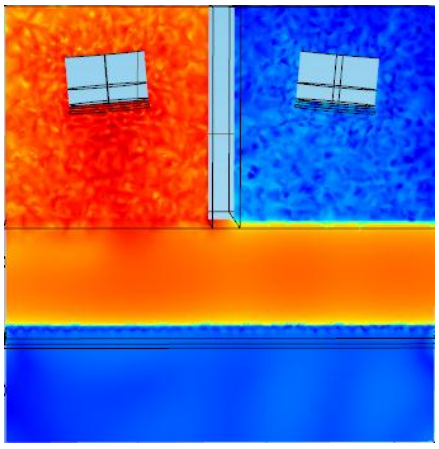

b. 200 V / 40 mm delamination [dB]

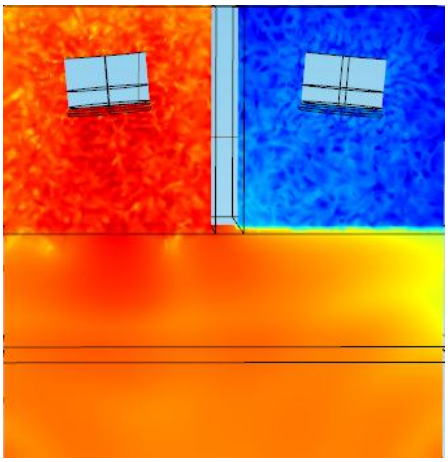

c. 300 V / no delamination [dB]

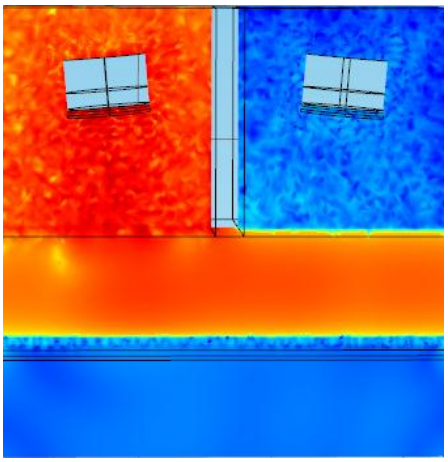

d. 300 V / 40 mm delamination [dB]

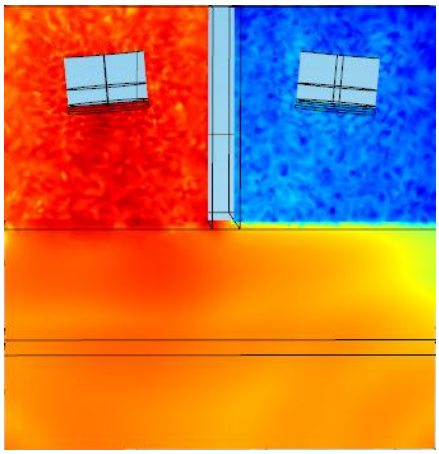

e. 400 V / no delamination [dB]

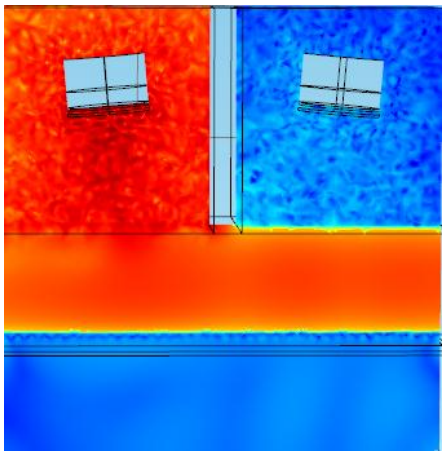

f. 400 V / 40 mm delamination [dB]

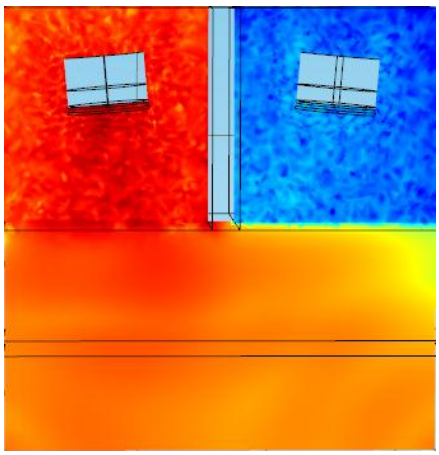

g. 500 V / no delamination [dB]

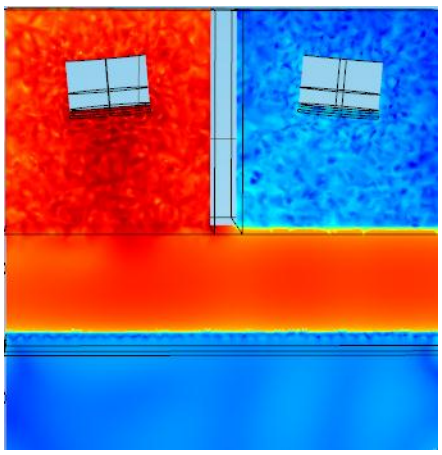

h. 500 V / 40 mm delamination [dB]

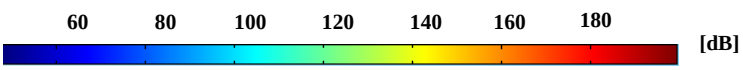

Figure 2.10 Investigation of the impact of the excitation voltage

2.4.5 CASE V: Angle of incidence study

The angle incidence study investigates the effects of moving the acoustic field across the model, which is a combination of longitudinal, transverse and surface waves. As the angle of incidence increases the type of wave, which dominates the effects of acoustic pressure at the receiver slowly changes. Because of this, the output of these test cases can only identify the angles at which acoustic pressure is at its peak. All parameters other than the angles are based on the near field test case "g".

The performed tests are as follows: (i) before the first critical angle: 3^0, (ii) between the first and second critical angles: 5^0 and 6^0, (iii) after the second critical angle: $6.9^0$and 9^0. Figures 2.11-12 present the simulation results in the case of variation of the angle of incidence from the defined critical angles: 4.93^0 and 6.93^0. As the transducer tends towards a perpendicular position with respect to the inspection surface, the difference in the impulse response between the cases with and without delamination is higher. At angles higher that the second limit, there is a total reflection of both longitudinal and transverse waves.

Angle of incidence study	
Active Area Diameter (mm)	30
Frequency (Hz)	75000
Angle (Degrees)	3 - 9
Near Field (mm)	41.1
Near Field Depth from Surface (mm)	0
First Critical Angle (Degrees)	4.93
Second Critical Angle (Degrees)	6.93
Delamination Depth (mm)	-40
Inspection depth (mm)	-40
Transducer Separation (mm)	90.76
Height from surface (mm)	39.85
Excitation voltage (V)	300

a. Case setup

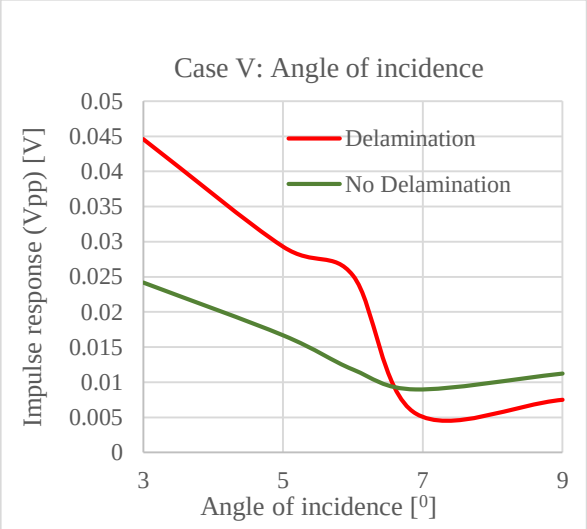

b. Angle of incidence vs. Impulse response at the receiver (Vpp)

Figure 2.11 Investigation of the impact of the angle of incidence

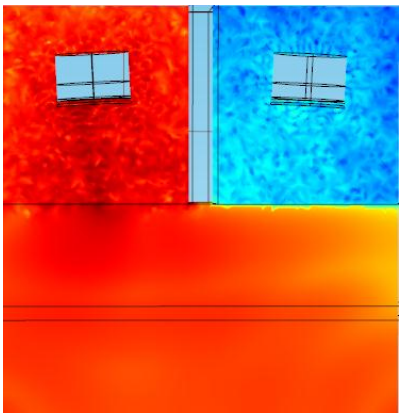

a. 3^0 angle of incidence / no delamination [dB]

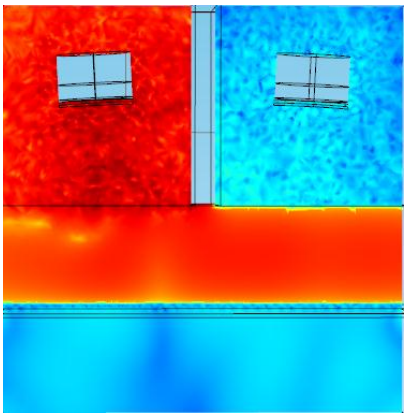

b. 3^0 angle of incidence / 40 mm delamination [dB]

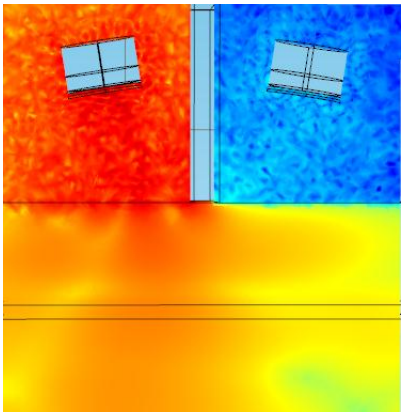

c. 5^0 angle of incidence / no delamination [dB]

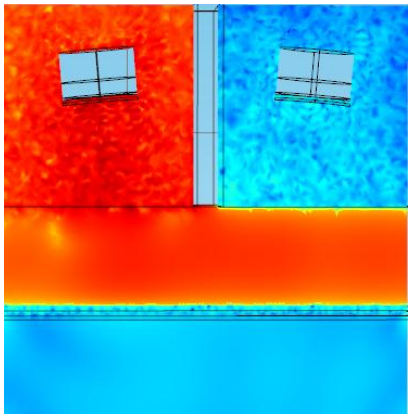

d. 5^0 angle of incidence / 40 mm delamination [dB]

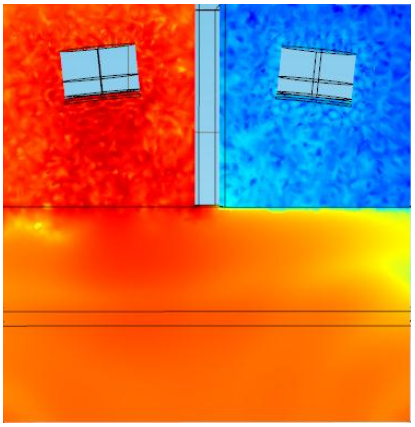

e. 6^0 angle of incidence / no delamination [dB]

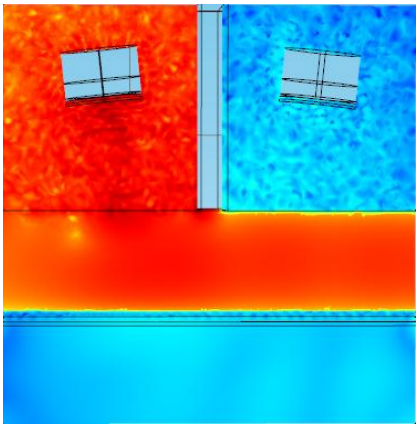

f. 6^0 angle of incidence / 40 mm delamination [dB]

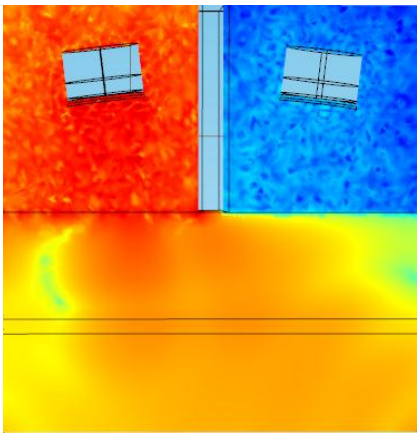

g. 6.9^0 angle of incidence / no delamination [dB]

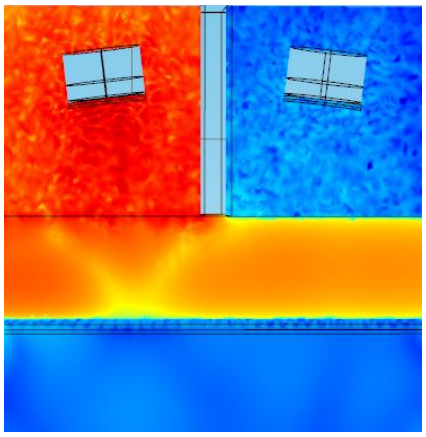

h. 6.9^0 angle of incidence /40 mm delamination [dB]

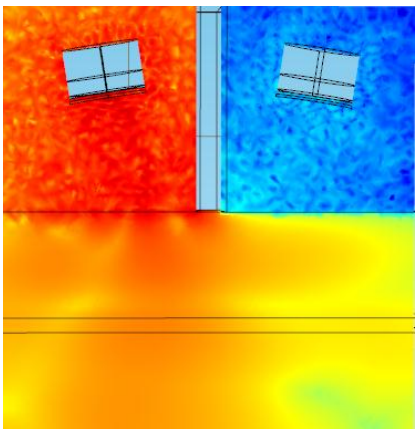

i. 9^0 angle of incidence / no delamination [dB]

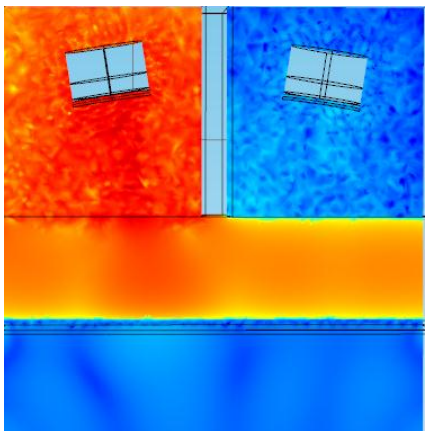

j. 9^0 angle of incidence / 40 mm delamination [dB]

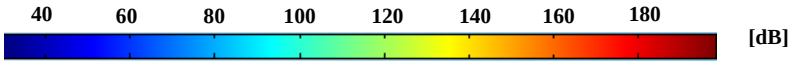

Figure 2.12 Investigation of the impact of the angle of incidence

2.4.6 CASE VI: Detection of subsurface delaminations

The subsurface delamination case study evaluates the system's ability to detect various types of delaminations at different depths based on the geometrical system configuration used for the near field test case "g". As can be seen from the computed acoustic pressure levels and taking into account the additional impact of the bituminous membrane (40 mm depth), it is evident that there are regions where there is a decrease in the contrast between the impulse response for the cases with and without delamination, as the depth of the delamination increases.

Delamination depth study	
Active Area Diameter (mm)	30
Frequency (Hz)	75000
Angle (Degrees)	5
Near Field (mm)	41.1
Near Field Depth from Surface (mm)	0
First Critical Angle (Degrees)	4.93
Second Critical Angle (Degrees)	6.93
Delamination Depth (mm)	-40
Inspection depth (mm)	-40
Transducer Separation (mm)	90.76
Height from surface (mm)	39.85
Excitation voltage (V)	300

a. Case setup

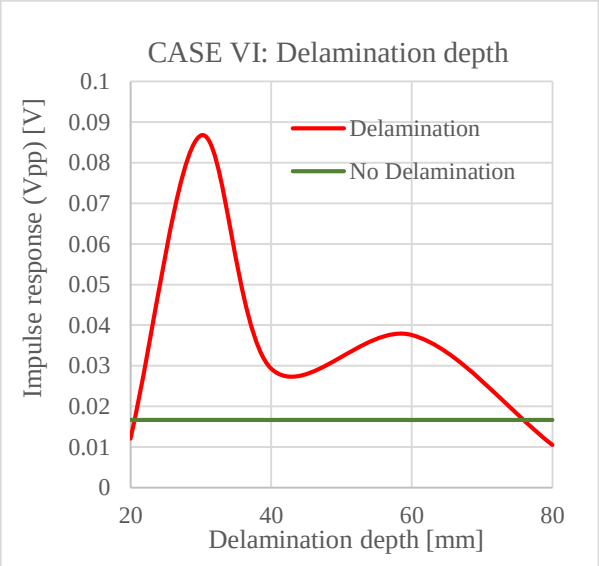

b. Delamination depth vs. Impulse response at the receiver (Vpp)

Figure 2.13 Investigation of the delamination depth

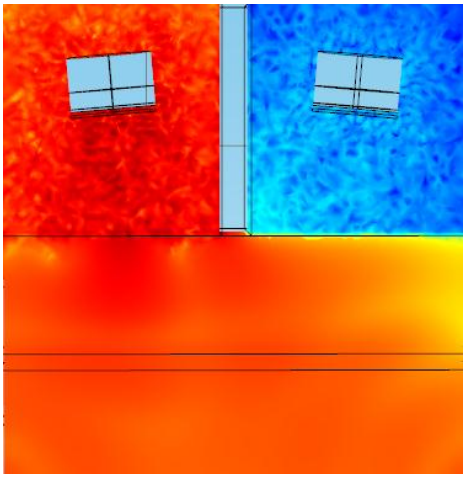

a. no delamination [dB]

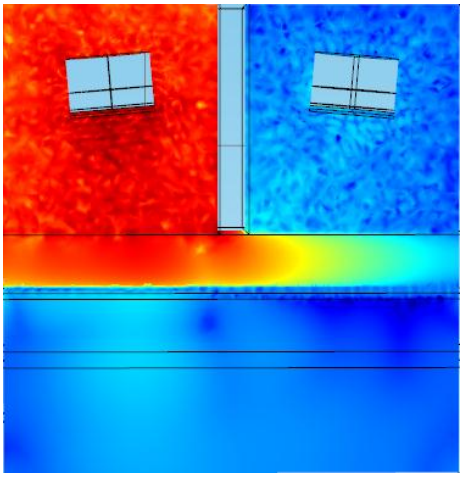

b. 20mm depth delamination / air-filled / 2 mm height [dB]

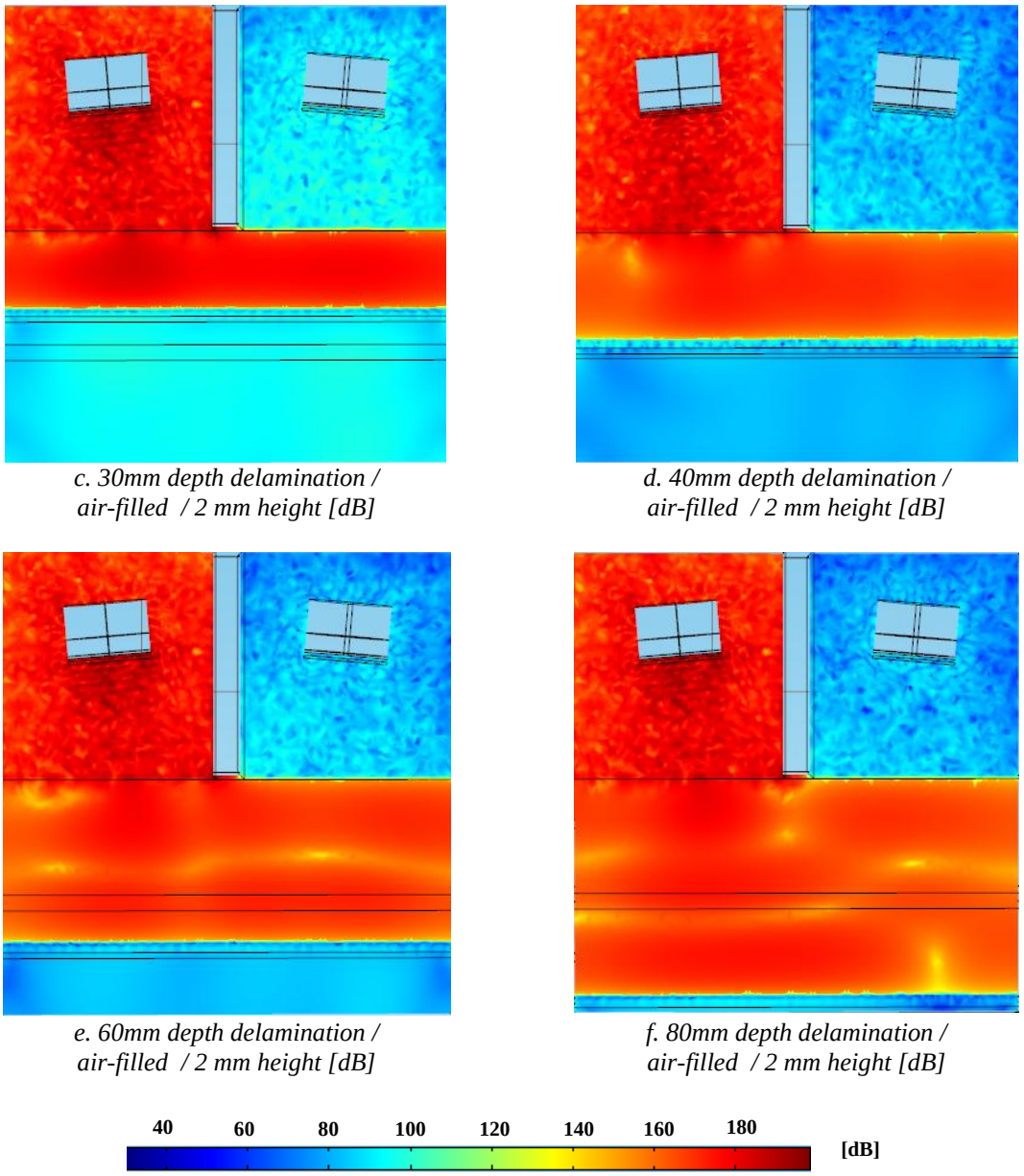

c. 30mm depth delamination / air-filled / 2 mm height [dB]

d. 40mm depth delamination / air-filled / 2 mm height [dB]

e. 60mm depth delamination / air-filled / 2 mm height [dB]

f. 80mm depth delamination / air-filled / 2 mm height [dB]

Figure 2.14 Computed acoustic pressure levels for delaminations of varying depth

Figure 2.15 shows the comparison of the computed acoustic pressure levels for various delamination types: air-filled, water-filled, and low density HMA (modelled stripping defect). As can be observed in Figure 2.15.a, the water filled delamination and the areas of low-density stripping produce even higher impulse response in comparison to the air-filled 2mm height delamination. This may also indicate that assessment of delamination volume or multiple subsurface defects is quite challenging.

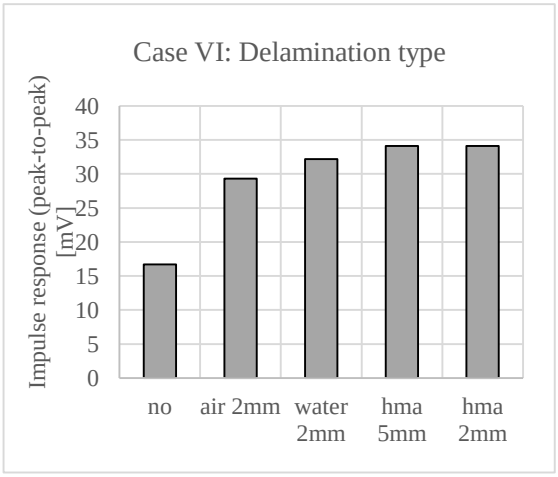

a. Delamination type vs. Impulse response

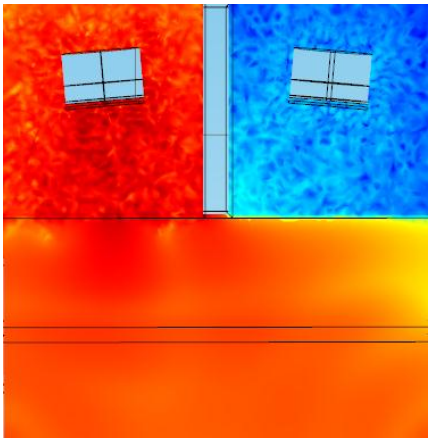

b. no delamination [dB]

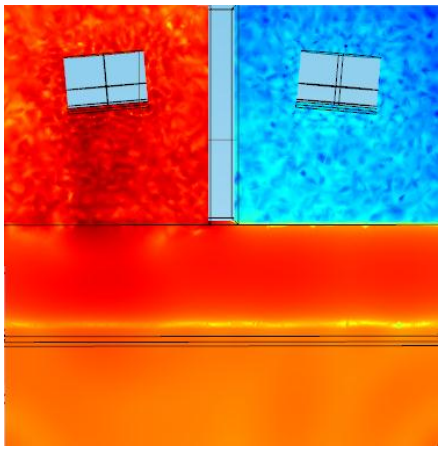

a. 40mm depth delamination / water-filled / 2mm height [dB]

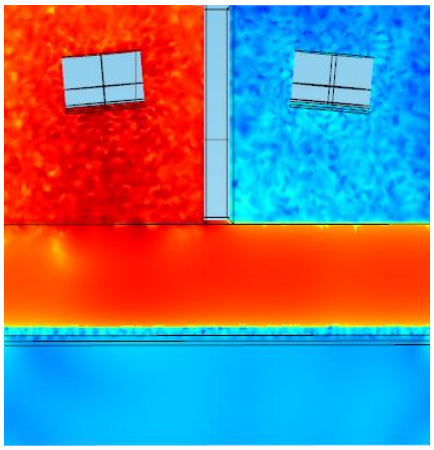

b. 40mm delamination / air-filled / 2 mm height [dB]

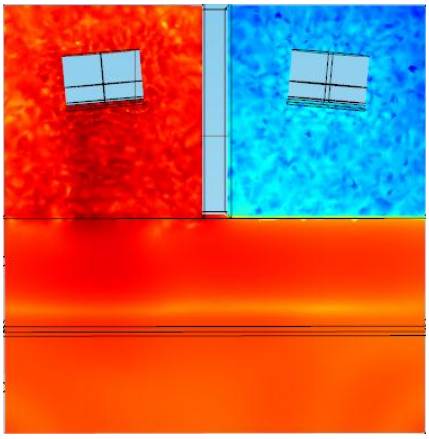

c. 40mm depth delamination / low density HMA / 2mm height [dB]

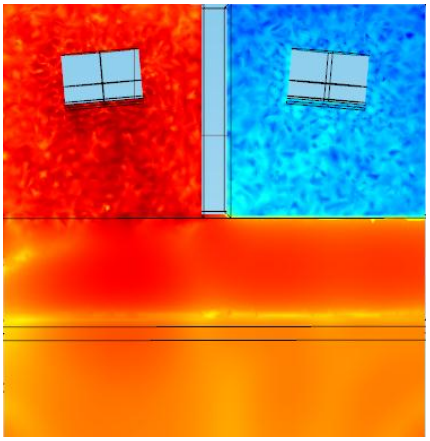

d. 40mm depth delamination / low density HMA / 5mm height [dB]

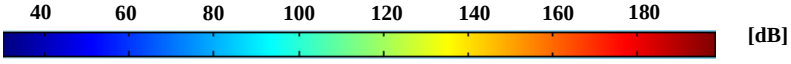

Figure 2.15 Computed acoustic pressure levels for cases with delaminations of various types

2.4.7 CASE VII: Impact of surface defects

Figures 2.16-17 present the simulation results for the cases of two surface opening cracks 2x7mm and 7x10 mm in size and a 30x10 mm pothole. It can be observed from both the computed acoustic pressure levels and Vpp at the receiver that while there is a sufficient difference in the cases with/without delamination, the system is sensitive to surface defects, which can lead to erroneous interpretation of the results for subsurface delaminations. At the same time, the system may be able to indicate the presence of a surface defect. This case study requires thorough investigation during the laboratory testing phase.

Impact of surface defects study	
Active Area Diameter (mm)	30
Frequency (Hz)	75000
Angle (Degrees)	5
Near Field (mm)	41.1
Near Field Depth from Surface (mm)	0
First Critical Angle (Degrees)	4.93
Second Critical Angle (Degrees)	6.93
Delamination Depth (mm)	-40
Inspection depth (mm)	-40
Transducer Separation (mm)	90.76
Height from surface (mm)	39.85
Excitation voltage (V)	200

a. Case setup

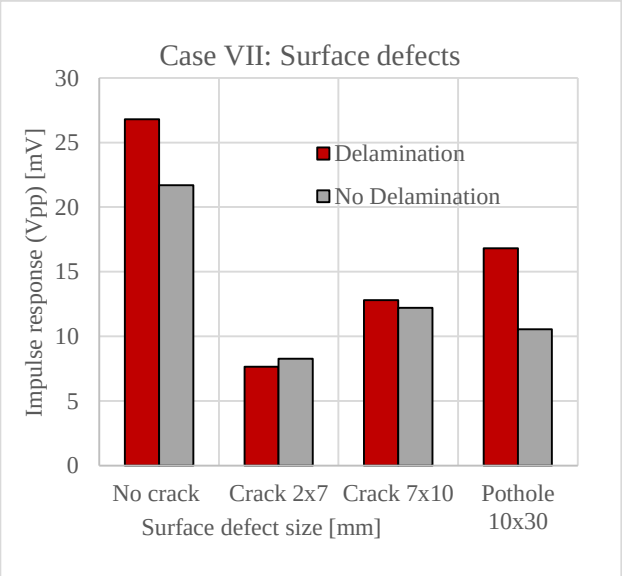

b. Presence of surface defects vs. Impulse response at the receiver (Vpp)

Figure 2.16 Investigation of the impact of surface defects

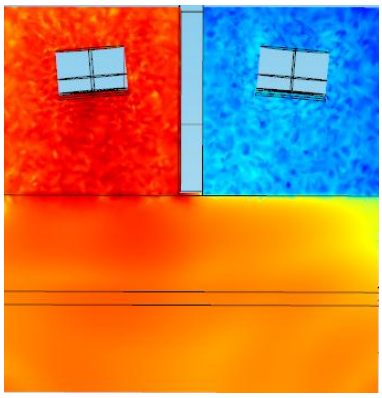

a. no surface defects / no delamination [dB]

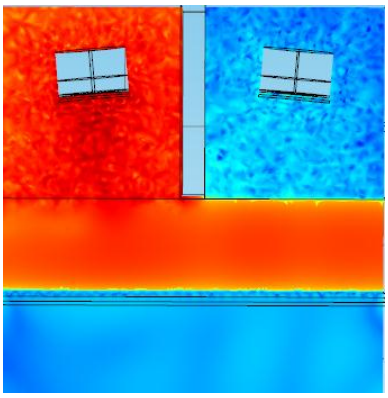

b. no surface defects / 40mm depth delamination [dB]

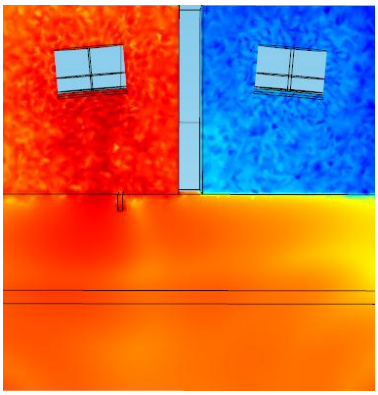

c.2x7mm surface crack / no delamination [dB]

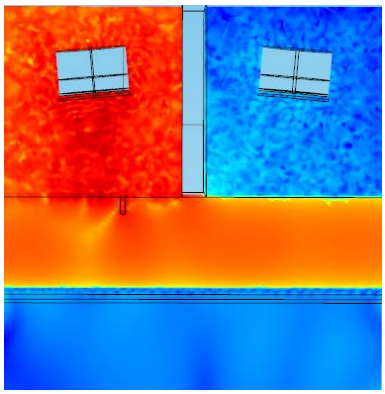

d. 2x7mm surface crack / 40mm depth delamination [dB]

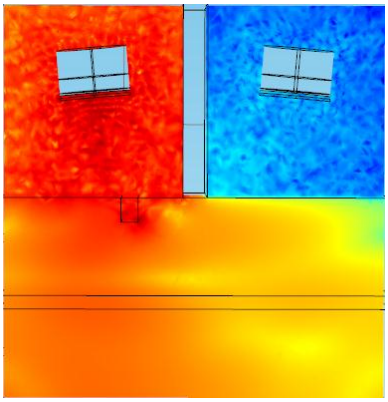

e. 7x10mm surface crack / no delamination [dB]

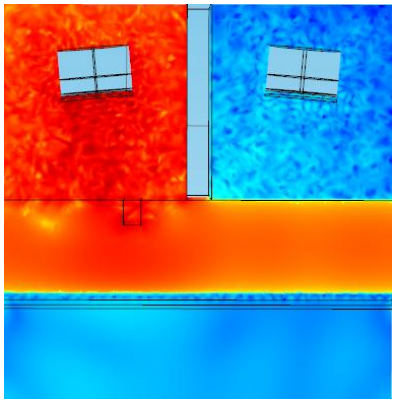

f. 7x10mm surface crack / 40mm depth delamination [dB]

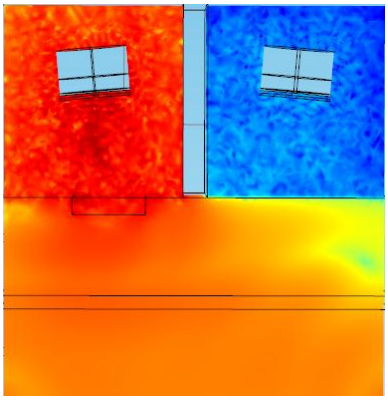

g. 30x10mm pothole/ no delamination [dB]

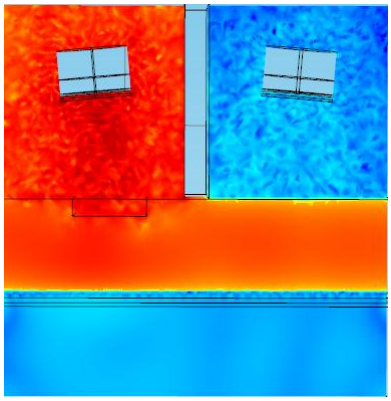

h. 30x10mm pothole / 40mm depth delamination [dB]

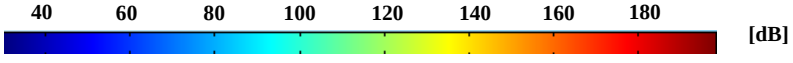

Figure 2.17 Computed acoustic pressure levels for cases with surface defects

2.4.8 CASE VIII: Impact of the shield position

As can be seen in Figure 2.18, the absence of the shield-surface contact significantly affects the acoustic pressure fields and consequently might lead to lower SNR. However, as the study was performed in the frequency domain, the impulse response with respect to the excitation pulse is the overlapping of all dispersed waves during the pulse period. Therefore, the system response in the time domain requires further investigation, which will be performed in due course and compared to the laboratory tests.

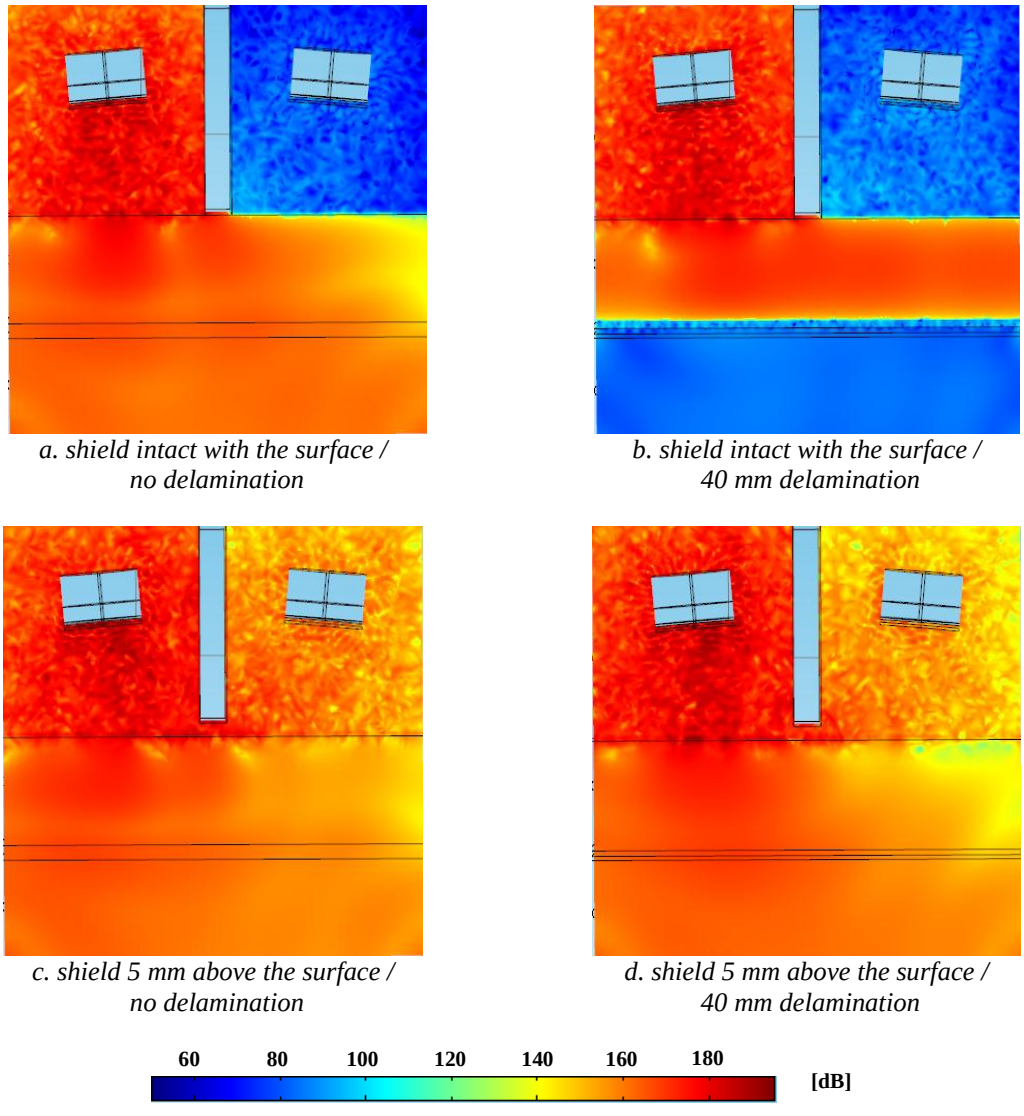

a. shield intact with the surface / no delamination

b. shield intact with the surface / 40 mm delamination

c. shield 5 mm above the surface / no delamination

d. shield 5 mm above the surface / 40 mm delamination

Figure 2.18 Investigation of the impact of the shield-surface distance

3 CONCLUSIONS

The aim of the development of the prototype system (Tasks 4.1, 4.2) consists of the specification and analysis of the ACU system's parameters and the assessment of the accuracy in the detection of shallow subsurface detects in concrete/HMA pavements.

Based on the definition of the general system specifications and guidelines, the results of the FEM-based parametric study showed how the choice of system parameters impacts on the interaction of the waves with the subsurface delaminations and the overall ACU system performance. The investigations included delamination depth/type, system geometrical configuration, inspection frequency, and excitation voltage. The impact of the pavement surface defects (i.e., surface opening cracks) on the ultrasonic wave propagation was also analysed.

The results indicated that the proposed system configuration is capable of detecting subsurface delaminations, subject to the following parameter considerations:

- The system should be implemented taking into account that the acoustic pressure significantly increases when the transducers are positioned closer to the inspection surface. This parameter should be kept to a minimum, however taking into account the geometric constraints of the environment and the transducer operational specifications.
- With respect to geometrical tolerances, the results indicate that as a transducer's angle of incidence decreases, the model becomes more sensitive to the transducer separation distance. At the same time, the angle has to lie between the first and second critical angle to maximise ultrasonic transmission.
- Similarly to what was shown by Gräfe [1] and Dunning [19], the simulation results confirm an optimal frequency of 75 kHz for ACU concrete and HMA inspection within the 60 mm depth range.
- Higher excitation voltage results in a higher impulse response and it is preferable to use the highest operational voltage.
- The simulation results demonstrated that detection of subsurface delaminations is achievable without the presence of surface defects with a higher impulse response difference within the 30-60 mm depth range.
- It has been indicated that various delamination types including air-filled, water-filled, and low density HMA (modelled stripping defects) produce a similar level of response. Under the existing modelling assumptions, the ACU should be able to identify the most common types of subsurface delaminations. However, assessment of delamination volume and presence of multiple subsurface defects require additional investigation.
- It can be observed from both the computed acoustic pressure levels and impulse response that, while there is sufficient difference in the cases with/without delamination, the system is sensitive to surface defects, which can lead to erroneous interpretation of the results for subsurface delaminations. At the same time, the system may be able to indicate the presence of a surface defect. This will require thorough investigation during the laboratory testing phase.
- The absence of the shield-surface contact significantly affects the computed acoustic pressure fields and consequently may lead to lower SNR.

In summary, appropriate choice and tuning of parameters may lead to ACU systems capable of overcoming the inherent issue of high impedance mismatch and should be effective in single-side HMA pavement inspection. In order to increase the ACU system's sensitivity to the subsurface defects, further investigation of the optimal geometric configuration during the laboratory testing of the equipment will be carried out.

During the system implementation stage, the general requirements for the pulser and processing of the received signal will be thoroughly analysed in combination with the post-processing mechanisms in the course of Tasks 4.2-3. In addition, the case of multiple transducer pair positioning for greater lateral coverage will be investigated.

REFERENCES

[1] B. Gräfe, "Luftgekoppeltes Ultraschallecho-Verfahren für Betonbauteile," PhD Thesis (in German), Technischen Universität Berlin, 2008.

[2] FEA COMSOL Acoustics Module manual: http://www.comsol.com/

[3] E. N. Mallory, "Nondestructive Testing Methods, Analyses and Applications," 2011, ISBN 1608761576.

[4] C. H. Chen, "Ultrasonic and Advanced Methods for Nondestructive Testing and Material Characterization," ISBN 9812704094

[5] Pietro Burrascano, Ultrasonic Nondestructive Evaluation Systems: Industrial Application Issues, 2014, ISBN 3319105655

[6] The Ultran Group: http://www.ultrangroup.com/

[7] DR.HILLGER NDT Systems: http://www.dr-hillger.de/

[8] Airstar Inc: http://www.airstar1.com/

[9] Imaginos NDE: http://www.imaginosnde.com/

[10] Japan Probe: http://www.jp-probe.com/

[11 Starmans Electronics: http://www.starmans.net/

[12] FP7 RPB HealTec, Deliverable D1.2 "System specifications", 2014.

[13] S. J. S. Martín, "Air-coupled ultrasound propagation and novel non-destructive bonding quality assessment of timber composites," PhD thesis, Department of Civil, Environmental and Geomatic Engineering Institute for Building Materials, Germany, 2012.

[14] E. Blomme, D. Bulcaen, and F. Declercq, "Air-coupled ultrasonic NDE: experiments in the frequency range 750 kHz ± 2 MHz," *NDT&E International*, vol. 35, pp. 417–426, 2002.

[15] H. B. Kichou, J. a. Chavez, a. Turo, J. Salazar, M. J. Garcia-Hernandez, and E. P. Tomasini, "Lamb Waves Amplitude Losses in Air-Coupled Ultrasonic NDT System due to the Beam Deviation Produced by Inclination of the Test Structure," *Proceedings of Ultrasonics International (UI'05) and World Congress on Ultrasonics (WCU)*, vol. 44, pp. 1077–1082, Dec. 2006.

[16] M. Schickert, "Ultrasonic techniques for evaluation of reinforced concrete structures," in *Non-Destructive Evaluation of Reinforced Concrete Structures: Non-destructive testing Methods. Vol. 2*, 2010, pp. 490–530.

[17] M. Dunning, M. Karakouzian, R.Y. Vun, M.C. Bhardwaj, "Non-contact ultrasonic characterization of hot mix asphalt," *Proc. of 16th World Conference on Nondestructive Testing*, , Montreal, Canada, Sep. 2004.

[18] J. Berriman, P. Purnell, D. a Hutchins, and a Neild, "Humidity and aggregate content correction factors for air-coupled ultrasonic evaluation of concrete.," *Ultrasonics*, vol. 43, no. 4, pp. 211–7, Feb. 2005.

[19] M. R. Dunning, "Feasibility for the use of non-contact ultrasound for application with asphalt concrete materials.," PhD Thesis, University of Nevada, Las Vegas, 2006.

[20] Application Note AN-305-4, SecondWave™ M510 Ultrasonic Analysis System, "Non-Contact Ultrasound analysis of concrete, highway, bridges, air strips," available online: http://www.ultrangroup.com/pdfexample/concrete.html

[21] Transportation Research Board, "NDT technology for quality assurance of HMA pavement construction", National Cooperative Highway Research Program, Report No. 626. Washington, DC: Transportation Research Board, 2009.

[22] P. Purnell, T. Gan, D. Hutchins, and J. Berriman, "Noncontact ultrasonic diagnostics in concrete: A preliminary investigation," *Cement and Concrete Research*, vol. 34, no. 7, pp. 1185–1188, Jul. 2004.

[23] S.H. Kee and J. Zhu, "Using air-coupled sensors to determine the depth of a surface-breaking crack in concrete.," *The Journal of the Acoustical Society of America*, vol. 127, no. 3, pp. 1279–87, Mar. 2010.

[24] CIVA NDT software: http://www-civa.cea.fr/en/civa-ndt-simulation-platform/ .

[25] W. Ke, M. Castaings, and C. Bacon, "3D finite element simulations of an air-coupled ultrasonic NDT system," *NDT & E International*, vol. 42, no. 6, pp. 524–533, Sep. 2009.

[26] G. Dobie, A. Spencer, K. Burnham, S. G. Pierce, K. Worden, W. Galbraith, and G. Hayward, "Simulation of ultrasonic lamb wave generation, propagation and detection for a reconfigurable air coupled scanner.," *Ultrasonics*, vol. 51, no. 3, pp. 258–69, Apr. 2011.

[27] D. Algernon, B. Gräfe, F. Mielentz, B. Köhler, and F. Schubert, "Imaging of the Elastic Wave Propagation in Concrete Using Scanning Techniques: Application for Impact-Echo and Ultrasonic Echo Methods," *Journal of Nondestructive Evaluation*, vol. 27, no. 1–3, pp. 83–97, Jul. 2008.